Supplementary Information

Molecular engineering of aggregation-induced emission enhanced photosensitizers to boost the theranostic performance in photodynamic therapy

Sauraj[a], Ji Hee Kang[a], O Hyun Lee[a], Anindita De[a], Dongyun Shin[a], Young Tag Ko[a]*

College of Pharmacy, Gachon University, Incheon, South Korea 21936

*Corresponding author:

Young Tag Ko

College of Pharmacy, Gachon University, Incheon, South Korea 21936

Tel.: +82-32-820-4923; fax: + 82-32-820-4829

E-mail address: youngtakko@gachon.ac.kr

Experimental Section:

Materials

4,4'-dimethoxybenzophenone, palladium(II) acetate, 4-vinylpyridine, 4-bromobenzophenone, tri(*o*-tolyl) phosphine, trimethylamine, 1,3,5-tris(bromomethyl)benzene, and rose bengal were purchased from Tokyo Chemical Industry (Tokyo, Japan). Titanium tetrachloride, zinc, 9,10-anthracenediyl-bis(methylene) dimalonic acid (ABDA), 2'-7'dichlorofluorescin diacetate (DCFH-DA), dihydrorhodamine 123 (DHR123), anhydrous tetrahydrofuran (THF), *N*, *N*-dimethylformamide (DMF), chloroform-d6, and all other chemicals were purchased from Sigma-Aldrich Chemical Co. (St. Louis, MO, USA) and used as received without further purification. Dulbecco's modified Eagle's medium (DMEM), and fetal bovine serum (FBS) were supplied from HyClone (Cytiva). 3-(4,5-dimethyl-2-thiazolyl)-2,5-diphenyltetrazolium bromide (MTT) were supplied from Sigma-Aldrich (St. Louis, MO, USA). 1,2-Distearoyl-*sn*-glycero-3-phosphoethanolamine-*N*-[methoxy(polyethylene glycol)-2000] (DSPE-PEG2000) was purchased from Avanti Polar Lipids (Alabaster, AL, USA).

Instruments

The ^{1}H NMR and ^{13}C NMR spectra were measured on Bruker Analytik (Karlsruhe, Germany). The samples were measured at 600 MHz in chloroform-d ($CDCl_3$). High-resolution mass spectra (HRMS) were recorded with a Finnegan MAT TSQ 7000 mass spectrometer system operating in a MALDI-TOF mode. UV–Vis absorption spectra were recorded using a Cary 60 UV-Vis spectrophotometer (Agilent Technologies Inc, Santa Clara, CA, USA) with a quartz cell. Fluorescence emission spectra of the samples were recorded using Cary Eclipse fluorescence spectrophotometer (Agilent Technologies Inc, Santa Clara, CA, USA). Hydrodynamic diameter was analysed by dynamic light scattering (DLS), using particle size analyser (ELSZ-1000, Otsuka Electronics Co, Osaka, 141 Japan).

Synthesis of AIE-PSs (TPEPyTMB-1, TPEPyTMB-2 and TPEPyTMB-3)

The synthesis of AIE-PSs was carried out according to scheme S1. Synthesis of TPE-Br (1): This compound was synthesized according to the previously reported method [1]. 4,4'-dimethoxybenzophenone (0.243g, 1mmol) and 4-bromobenzophenone (0.262 g, 1mmol) were dissolved in 10 ml dry THF followed by the addition of zinc powder (3.26 g, 5 mmol). The The suspension was cooled down to 0 ^{o}C, then titanium tetrachloride (2.0 ml) was added drop

wisely. After addition, the mixture was slowly warmed up to room temperature and then reflux at 80°C under argon atmosphere for 12h. After that, the mixture was cooled down in ice-water bath and (50 ml) saturated sodium bicarbonate aqueous solution was added slowly. The mixture was extracted with ethyl acetate (100 ml × 3) and the organic phase was washed with brine (100 ml × 2), and then dried over $MgSO_4$. The mixture was filtered and the filtrate was concentrated under reduced pressure. The residue was purified with chromatography (hexane/ethyl acetate = 90/10) to obtain the desire product as a white solid (0.220 g, 46.8% yield). ^{1}H NMR (600 MHz, $CDCl_3$) δ 7.22 (d, 2H), 7.10 (m, 3H), 7.00 (m, 2H), 6.87- 6.94 (m, 6H), 6.67 (d, *J* = 8.8 Hz, 2H), 6.63 (d, *J* = 8.8 Hz, 2H), 3.76 (s, 3H), 3.73 (3, 3H); ^{13}C NMR (151 MHz, $CDCl_3$) δ158.2, 158.0, 143.8, 143.1, 140.9, 137.8, 136.1, 135.9, 133.0, 132.5, 131.3, 130.8, 127.7, 126.2, 113.2, 113.0, 55.0; LC-MS, m/z: $[M+H]^+$calcd 470.08., found 470.30.

Synthesis of TPEPy (2)

TPE-Br (470 mg, 1 mmol), 4-vinylpyridine (108 mg, 1 mmol), palladium (II) acetate (22 mg, 0.1 mmol) and tri (o-tolyl) phosphine (31mg, 0.1 mmol) were dissolved in 10 ml dry DMF. After that, (0.2 ml) trimethylamine was added to reaction mixture and stirred at 110°C temperature for 12 h under argon atmosphere. After cooling down the reaction mixture to room temperature, the reaction was quenched by water (30 ml) and the mixture was extracted with ethyl acetate. The collected organic layer was washed by brine, dried over Na_2SO_4 and concentrated under reduced pressure. The desired residue was purified by column chromatography using n-hexane/ethyl acetate (1/1 v/v) as eluent to give the desired product TPEPy as a yellow solid (282 mg, 56.8 %). ^{1}H NMR (600 MHz, CDCl3) *δ* 8.55 (d, 2H), 7.32 (d, 2H), 7.29 (s, 1H), 7.27 (s, 1H), 7.23-7.19 (m, 1H), 7.14-7.09 (m, 3H), 7.05-7.03 (m, 4H), 6.98-6.91 (m, 5H), 6.69 - 6.61 (m, 4H), 3.75 (s, 3H), 3.74 (s, 3H). ^{13}C NMR (151 MHz, CDCl3) *δ* 158.4, 158.3, 150.2, 145.3, 145.0, 144.2, 141.0, 138.7, 136.4, 136.3, 133.9, 133.2, 132.8, 132.7, 132.0, 131.6, 127.9, 126.6, 126.4, 125.5, 120.9, 113.3, 55.2. LC-MS, m/z: $[M+H]^+$ calcd 496.2, found 496.2.

Synthesis of TPEPyTMB-1

TPEPy (0.1 mmol, 49.6 mg) and 1,3,5-tris(bromomethyl)benzene (0.1 mmol, 35.6 mg) were dissolved in 10 ml dry toluene, and the reaction mixture was stirred at 80°C for 12 h under argon atmosphere. The progress of the reaction was monitored by TCL. The red precipitate formed during the reaction was filtered, washed with diethyl ether, and dried at room

temperature (42 mg, 54.4 %). ^{1}H NMR (600 MHz, $CDCl_3$) δ 8.86-8.84 (d, 2H), 8.26-8.22 (d, 2H), 7.74-7.72 (d, 1H), 7.32 (d, 1H), 7.22-7.12 (m, 3H), 7.12-6.92 (m, 8H), 6.94-6.88 (m, 4H), 6.69-6.51 (m, 5H), 5.42 (s, 2H), 4.62-4.52 (m, 4H), 3.76-3.72 (m, 6H). ^{13}C NMR (151 MHz, $CDCl_3$) δ 158.4, 158.3, 152.2, 148.2, 144.6, 144.4, 142.2, 142.0, 140.0, 138.7, 136.4, 136.3, 133.9, 133.2, 132.8, 132.7, 129.4, 129.2, 127.9, 126.6, 124.4, 122.5, 113.9, 113.3, 62.0, 55.2,32.2. HRMS (ESI), m/z: calcd for $C_{44}H_{38}NO_2Br_2$ $[M-Br]^+$ 772.60, found: 772.2412.

Synthesis of TPEPyTMB-2

The synthesis of TPEPyTMB-2 was carried out in the same manner by varying the molar ratio of TPEPy as (0.2 mmol, 99.2 mg), and the pure TPEPyTMB-2 was isolated as red powder (58.2 mg, 48.9 %). ^{1}H NMR (600 MHz, $CDCl_3$) δ 9.12-9.05 (m, 4H), 8.24-8.12 (m, 4H), 7.74-7.65 (dd, 2H), 7.32 (dd, 2H), 7.31-7.29 (m, 3H), 7.26-7.12 (m, 16H), 6.91-6.86 (m, 8H), 6.78-6.72 (m, 10H), 5.75-5.72 (m, 4H), 4.51 (s, 2H), 3.68-3.62 (m, 12H). ^{13}C NMR (151 MHz, $CDCl_3$) δ 158.4, 158.3, 150.2, 145.3, 145.0, 144.2, 141.0, 138.7, 136.4, 136.3, 133.9, 133.2, 132.8, 132.7, 132.0, 131.6, 127.9, 126.6, 126.4, 125.5, 120.9, 113.3, 65.2, 62.0, 55.2, 32.0. HRMS (ESI), m/z: calcd for $C_{79}H_{67}N_2O_4Br$ $[M-2Br]^+$ 1188.32, found: 1188.3825.

Synthesis of TPEPyTMB-3

The synthesis of TPEPyTMB-3 was carried out in the same manner by varying the molar ratio of TPEPy as (0.3 mmol, 148.8 mg), and the pure TPEPyTMB-3 was isolated as red powder (68 mg, 42.5 %). ^{1}H NMR (600 MHz, $CDCl_3$) δ 9.12-9.04 (m, 6H), 8.32-8.24 (m, 6H), 7.58-7.52 (3, 3H), 7.32-7.31 (m, 3H), 7.30-7.28 (m, 3H), 7.18-6.92 (m, 24H), 6.88-6.82 (m, 15H), 6.74-6.72 (m, 12H), 5.74-5.72 (m, 6H), 3.68-3.62 (m, 18H). ^{13}C NMR (151 MHz, $CDCl_3$) δ 158.4, 158.3, 150.2, 145.3, 145.0, 144.2, 141.0, 138.7, 136.4, 136.3, 133.9, 133.2, 132.8, 132.7, 132.0, 131.6, 127.9, 126.6, 126.4, 125.5, 120.9, 1132.8, 113.3, 62.2, 55.2. HRMS (ESI), m/z: calcd for $C_{114}H_{96}N_3O_6$ $[M-3Br]^+$ 1602.19, found: 1602.5463.

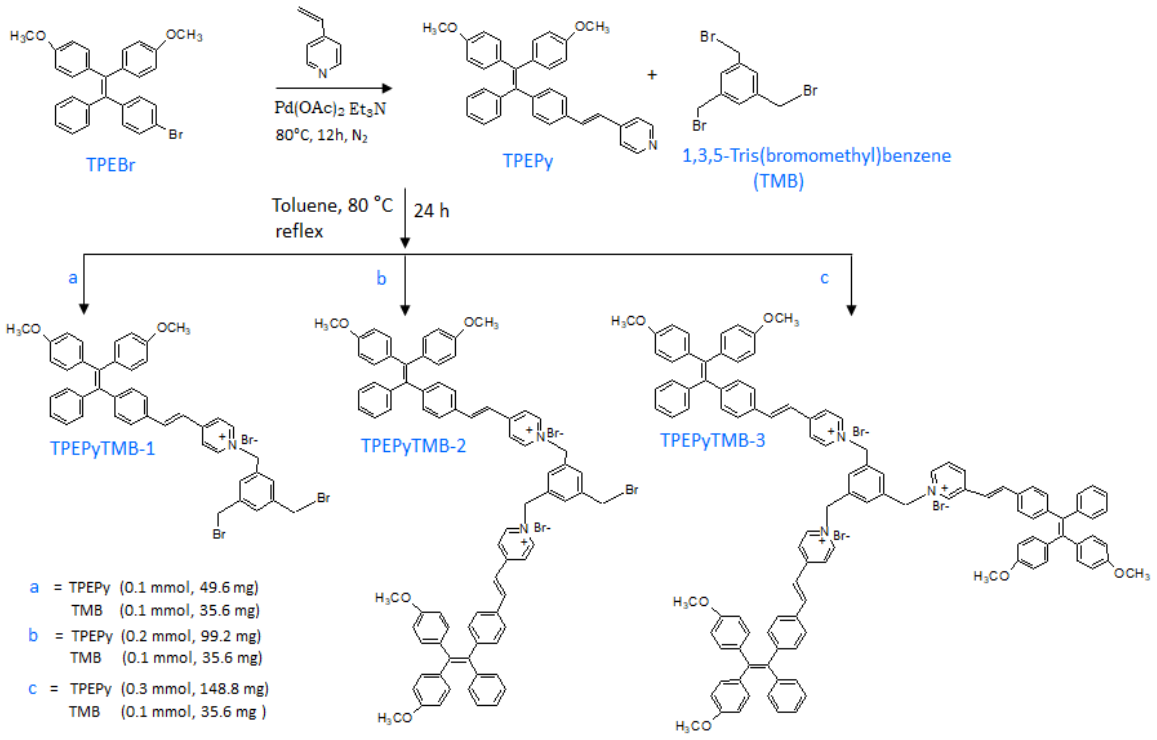

Scheme S1. Synthetic routes of TPEPyTMB-1, TPEPyTMB-2, and TPEPyTMB-3

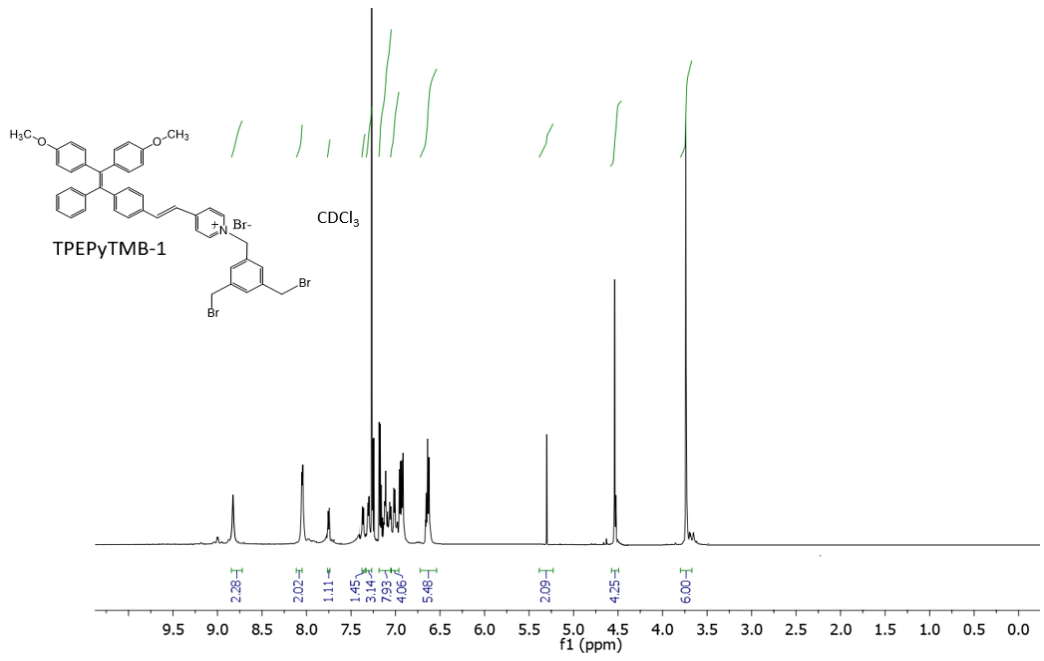

Fig. S1. ^{1}H NMR spectrum of TPEPyTMB-1

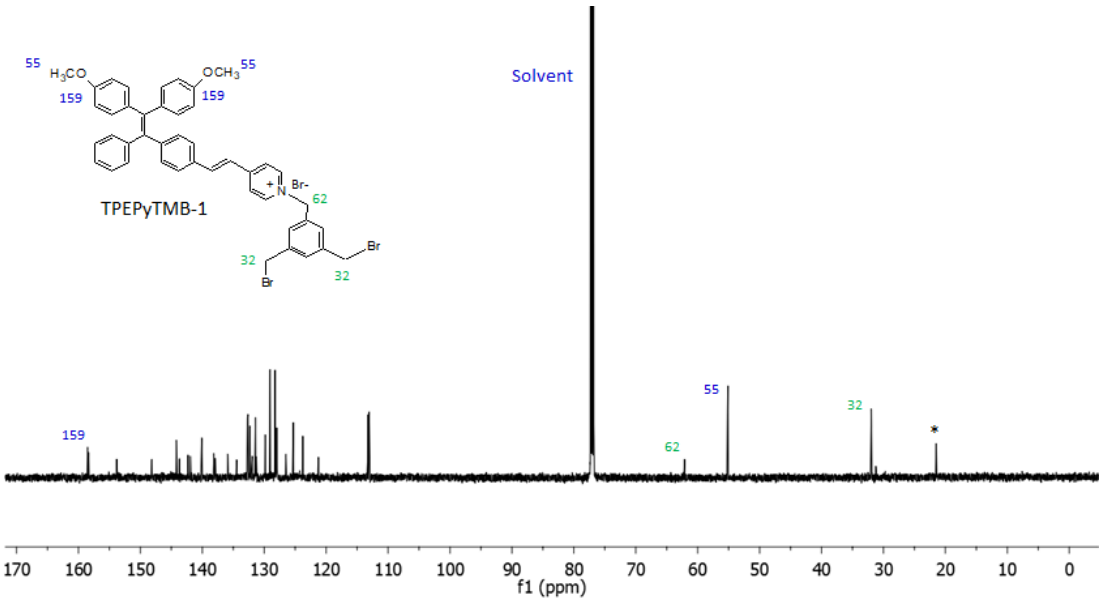

Fig. S2. ^{13}C NMR spectrum of TPEPyTMB-1

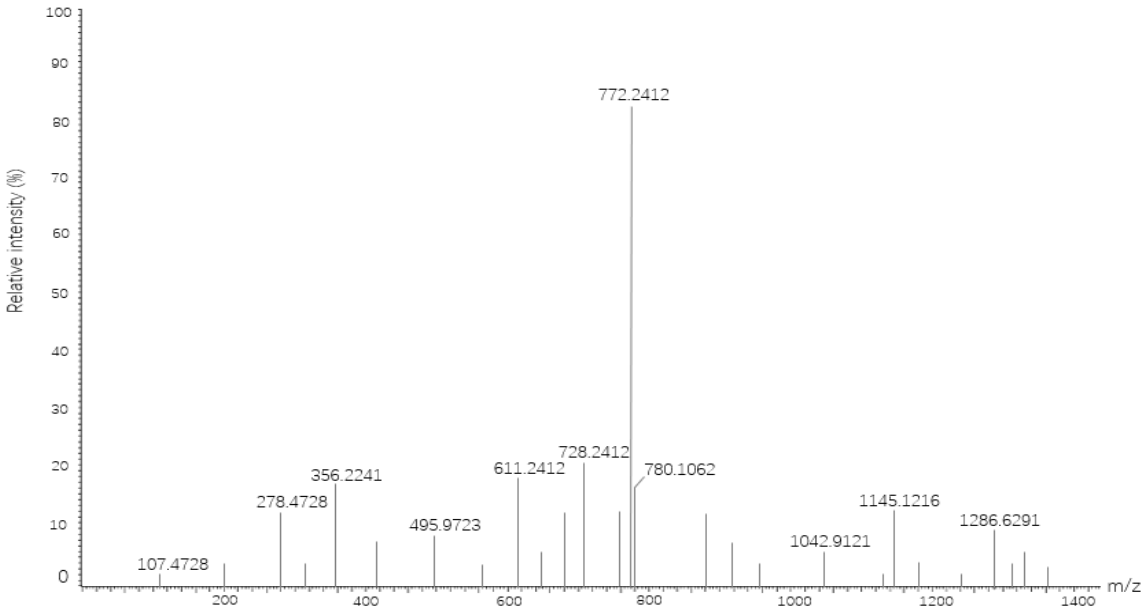

Fig. S3. HRMS spectrum of TPEPyTMB-1

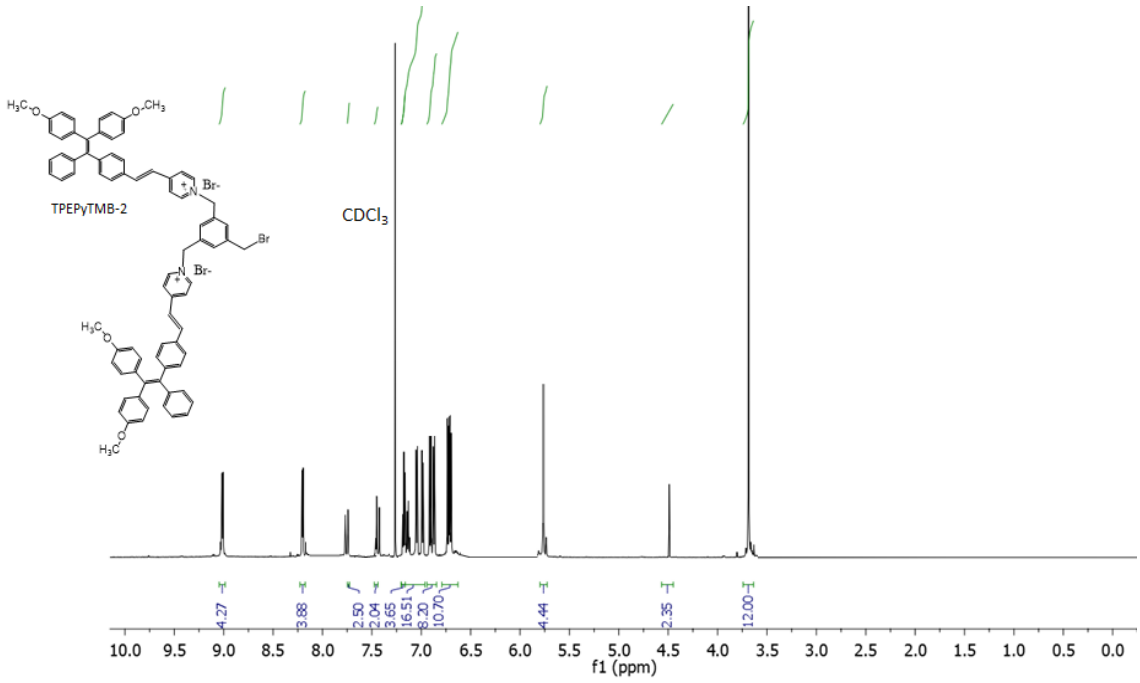

Fig. S4. [1]H NMR spectrum of TPEPyTMB-2

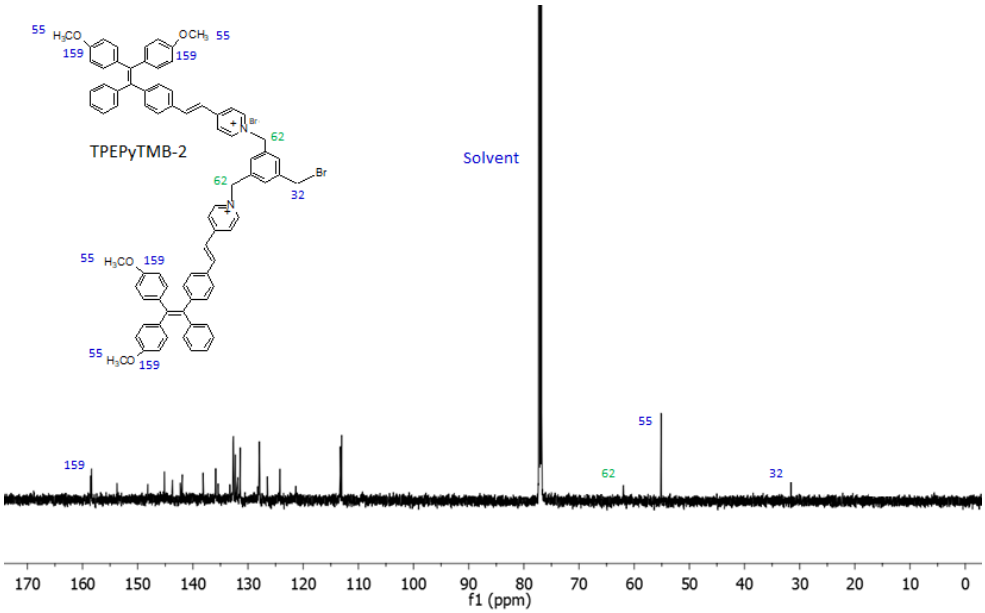

Fig. S5. [13]C NMR spectrum of TPEPyTMB-2

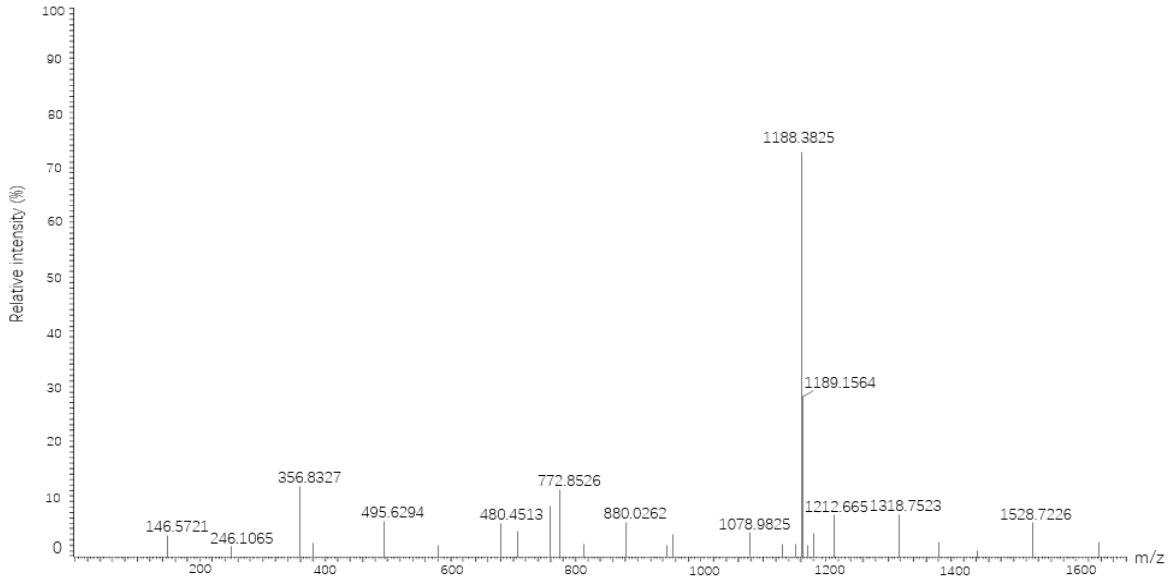

Fig. S6. HRMS spectrum of TPEPyTMB-2

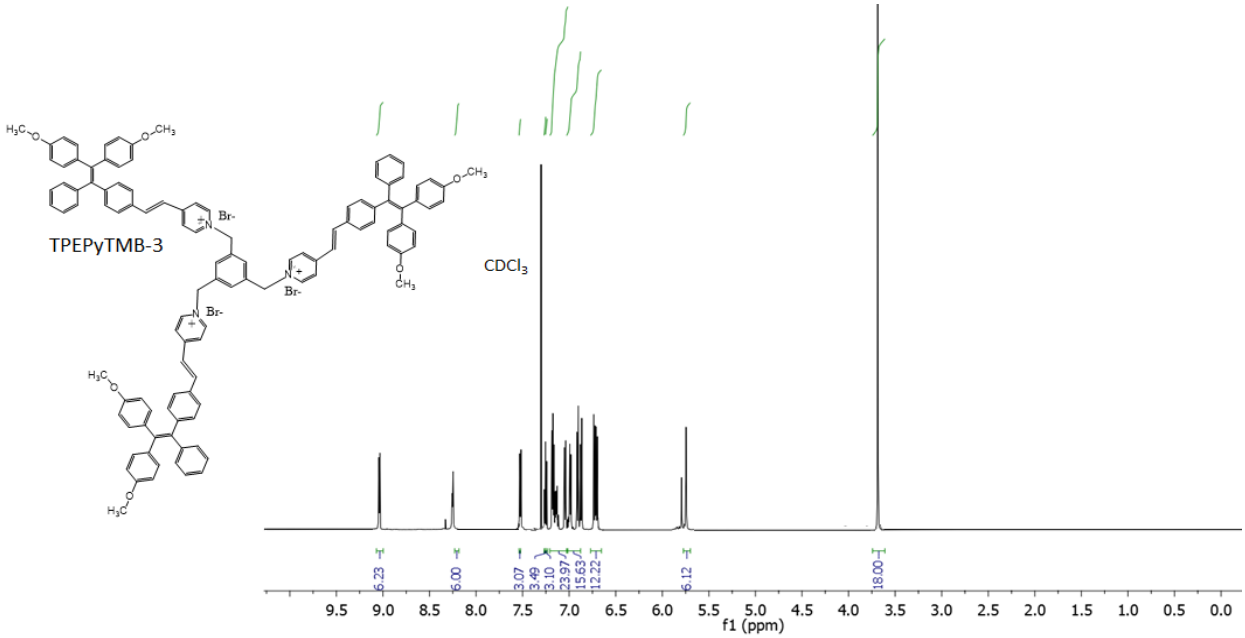

Fig. S7. ^{1}H NMR spectrum of TPEPyTMB-3

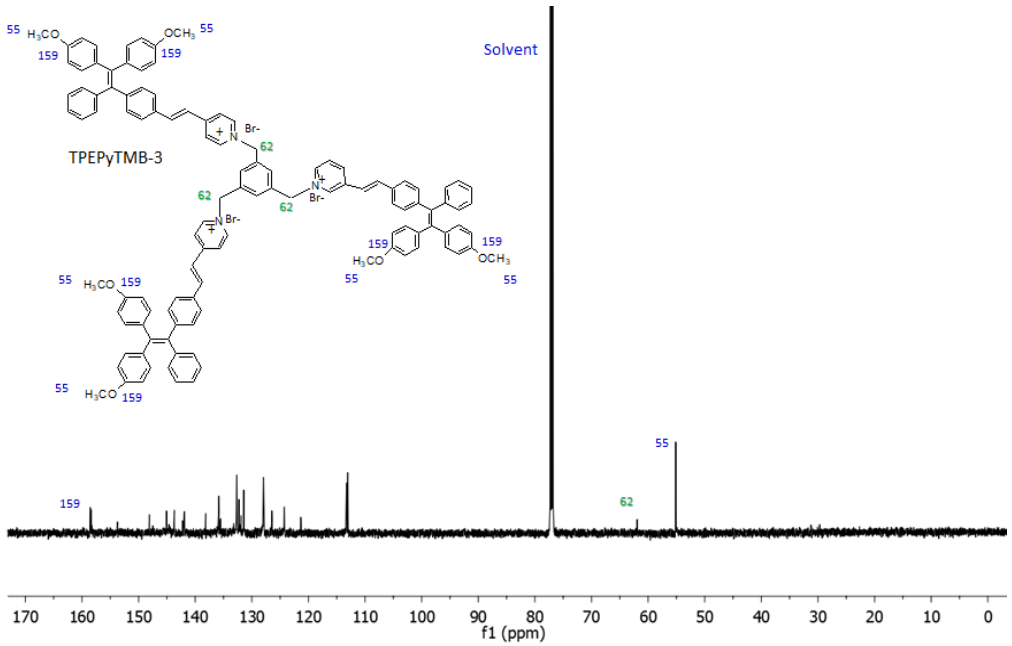

Fig. S8. ^{13}C NMR spectrum of TPEPyTMB-3

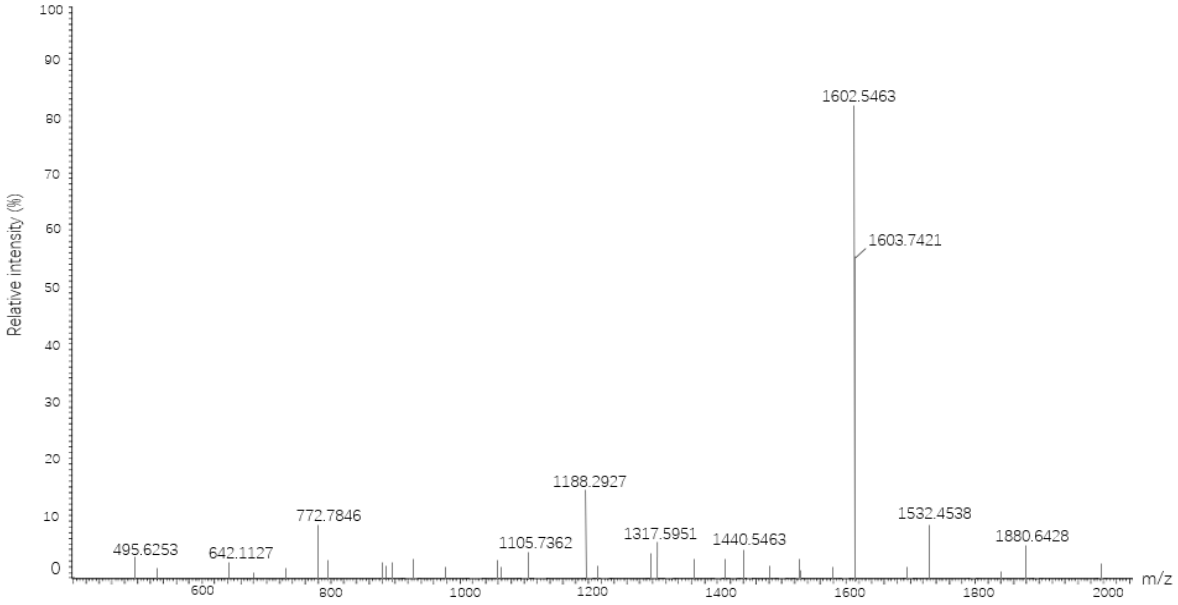

Fig. S9. HRMS spectrum of TPEPyTMB-3

Table S1. Photophysical properties of AIE-PSs NPs

Sample	Absorbance/Emission	Particle size (nm)	PDI	Zeta potential	Φ_F
TPEPyTMB-1 NPs	422/644	115.0 ± 1.32 nm	0.22 ± 0.24	-7.8 mV	8.49 %
TPEPyTMB-2 NPs	425/645	119.9 ± 6.12 nm	0.25 ± 0.24	-10.4 mV	11.81%
TPEPyTMB-3 NPs	427/648	125.2 ±4.42	0.28 ± 0.16	-11.8 mV	15.08%

nm

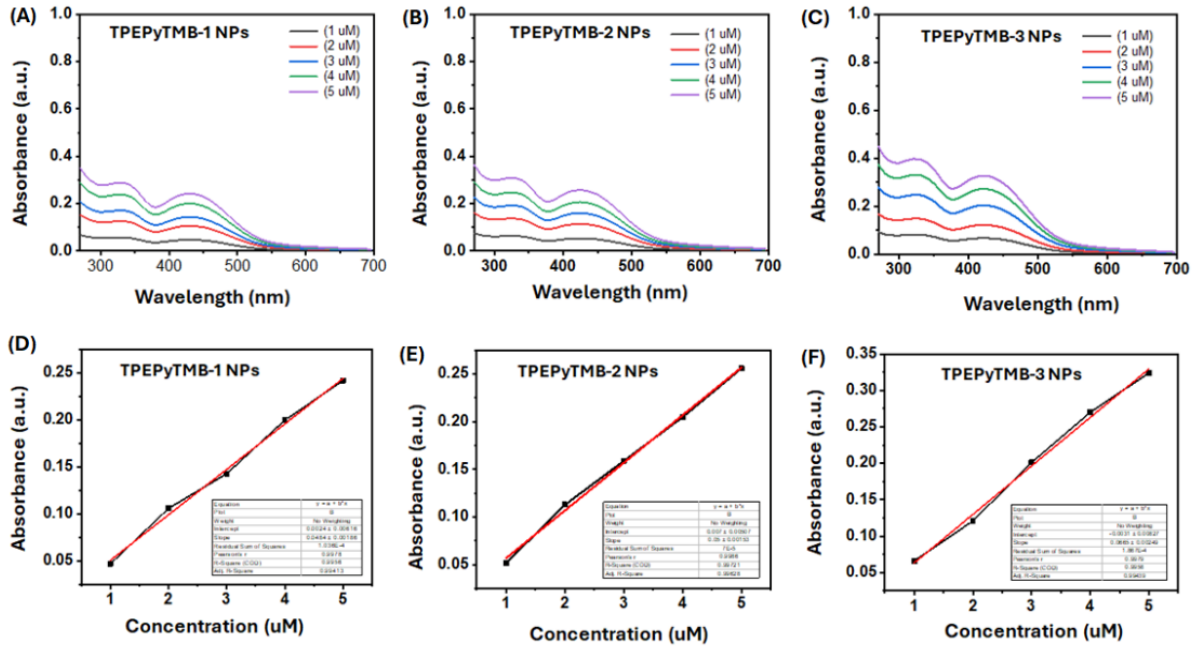

Fig. S10. (A-C) Absorbance of TPEPyTMB-1 NPs, TPEPyTMB-2 NPs, and TPEPyTMB-3 NPs in PBS (pH 7.4) at different concentrations, (d-f) Molar absorption coefficient of TPEPyTMB-1 NPs, TPEPyTMB-2 NPs, and TPEPyTMB-3 NPs measured in PBS (pH 7.4).

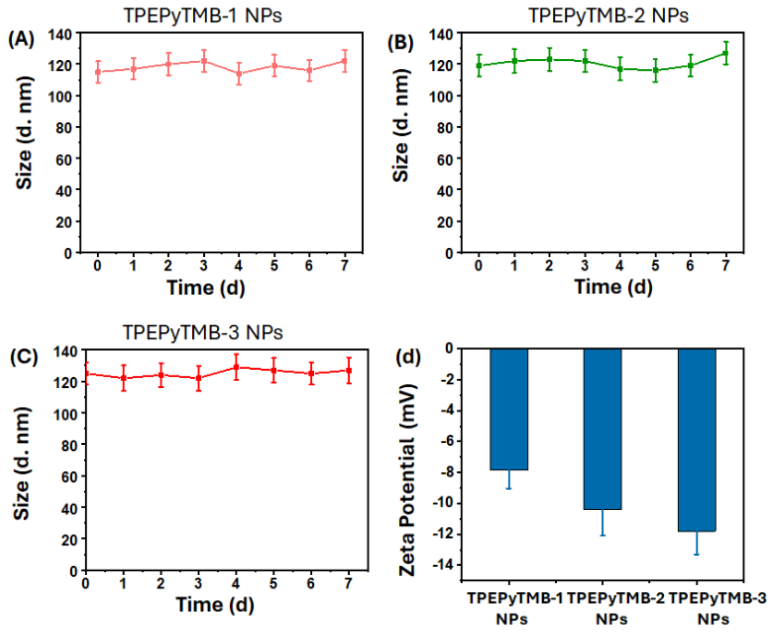

Fig. S11. (A-C) Stability of TPEPyTMB-1 NPs, TPEPyTMB-2 NPs, and TPEPyTMB-3 NPs in PBS (pH 7.4) for 7 days, and (D) Zeta potential of TPEPyTMB-1 NPs, TPEPyTMB-2 NPs, and TPEPyTMB-3 NPs measured in PBS (pH 7.4).

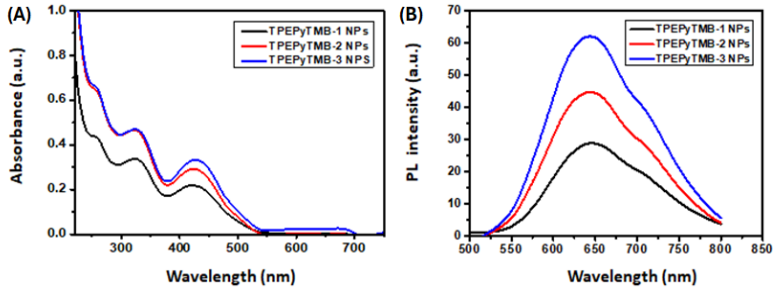

Fig. S12. (a) UV-Vis spectra of TPEPyTMB-1 NPs, TPEPyTMB-2 NPs, and TPEPyTMB-3 NPs, and (b) PL spectra of TPEPyTMB-1 NPs, TPEPyTMB-2 NPs, and TPEPyTMB-3 NPs in PBS (pH 7.4).

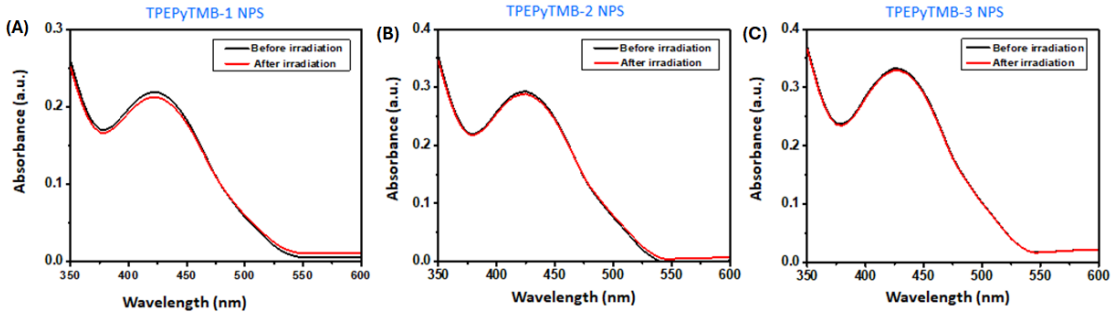

Fig. S13. Normalised absorption spectra of (a) TPEPyTMB-1 NPs, (b) TPEPyTMB-2 NPs, and (c) TPEPyTMB-3 NPs before and after irradiation.

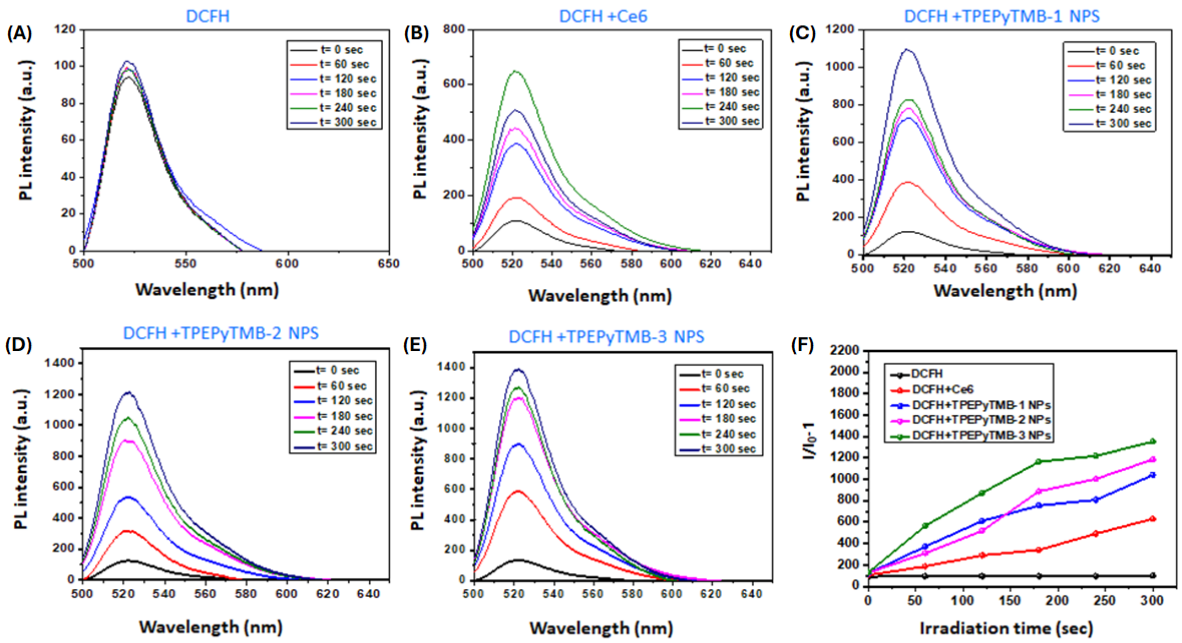

Fig. S14. PL spectra of (a) DCFH (5 μM), (b) DCFH +Ce6 (10 μM), (c) DCFH +TPEPyTMB-1 NPs (10 μM), (d) DCFH+TPEPyTMB-2 NPs (10μM), (e) DCFH +TPEPyTMB-3 NPs (10 μM) upon white light (100 mW/cm^2) irradiation and (f) relative ROS generation efficiency of AIE-PSs NPs and Ce6.

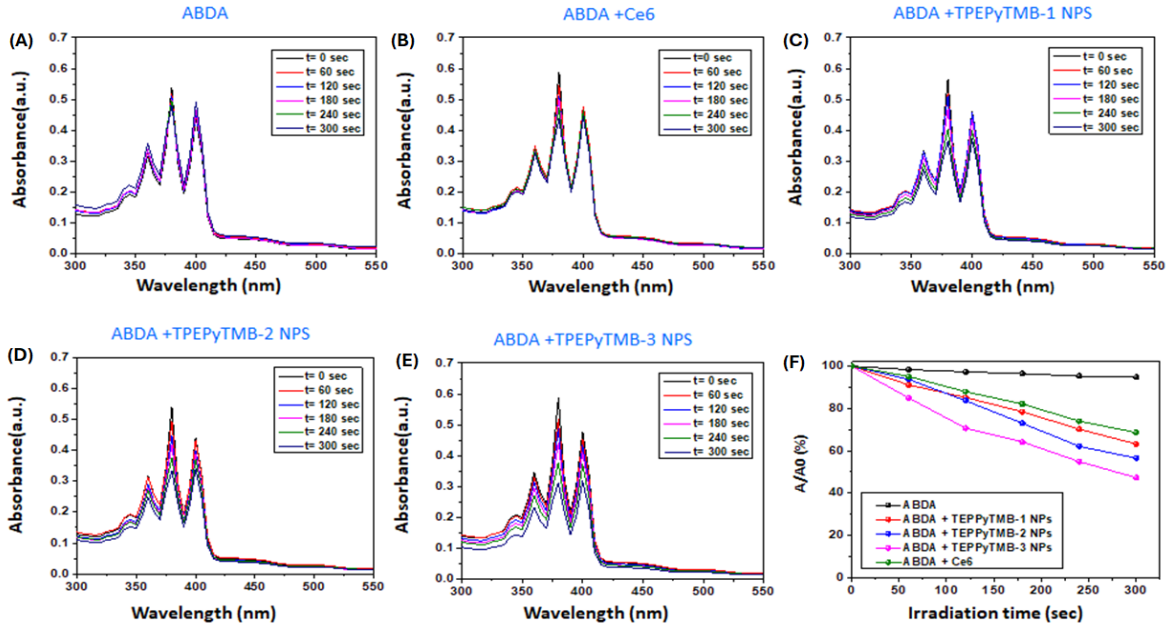

Fig. S15. Absorption spectra of (a) ABDA (5 μM), (b) ABDA+Ce6 (10 μM), (c) ABDA +TPEPyTMB-1 NPs (10 μM), (d) ABDA+TPEPyTMB-2 NPs (10μM), (e) ABDA+TPEPyTMB-3 NPs (10 μM) upon white light (100 mW/ cm^2) irradiation and (f) relative $^1O_2$ generation efficiency of AIE-PSs NPs and Ce6.

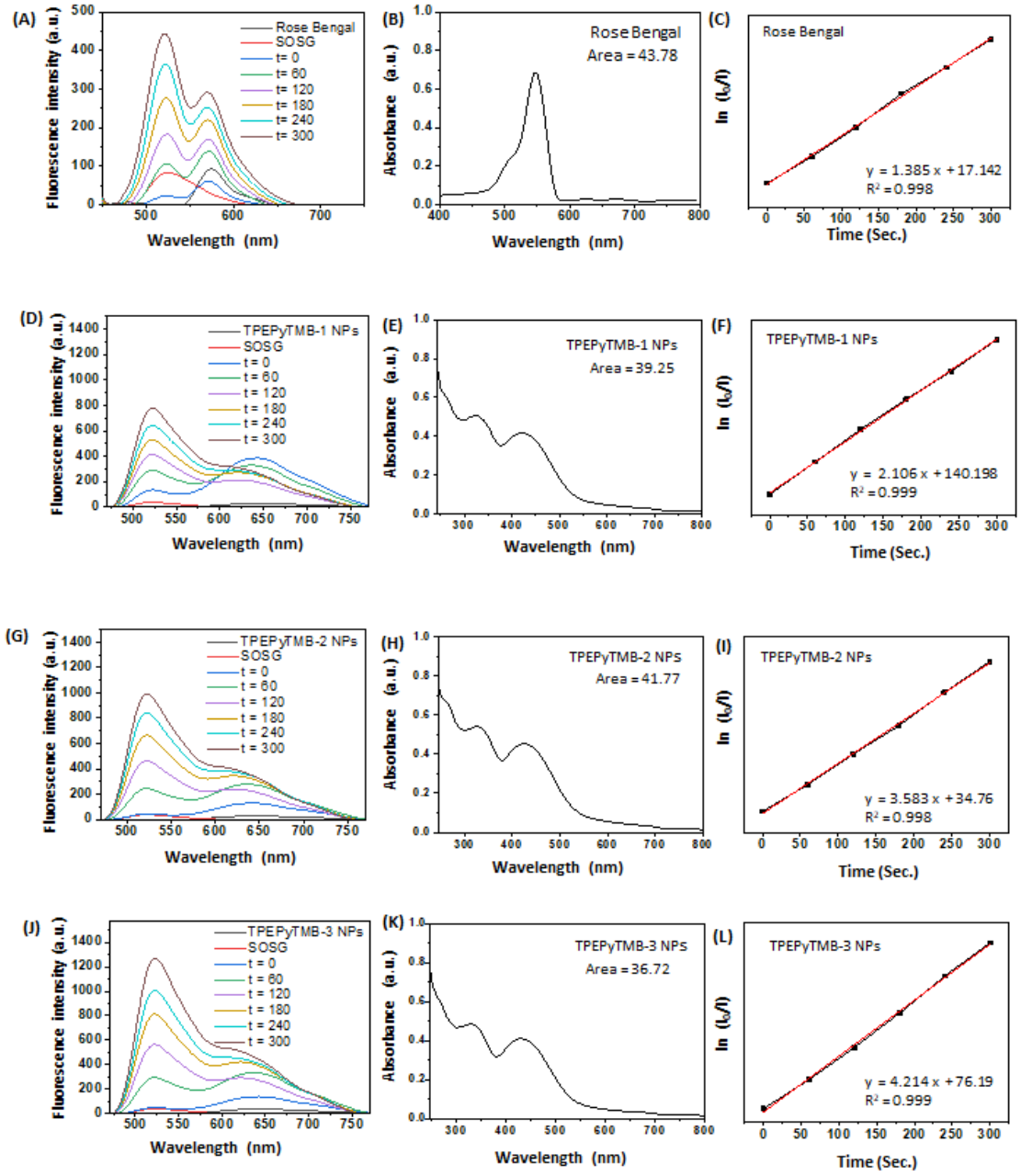

Fig. S16. Measurements of the $^1O_2$ quantum yield. Fluorescence intensity of SOSG (5μM) with (A) Rose Bengal (10 μM), (D)TPEPyTMB-1NPs (10 μM), (G) TPEPyTMB-2 NPs (10 μM), and (J)TPEPyTMB-3 NPs (10 μM). The absorption peak area of (B) RB, (E) TPEPyTMB-1NPs, (H) TPEPyTMB-2 NPs, and (K) TPEPyTMB-3 NPs. Rate constants of SOSG by (C) RB, (F) TPEPyTMB-1NPs, (I) TPEPyTMB-2 NPs, and (L) TPEPyTMB-3 NPs, respectively.

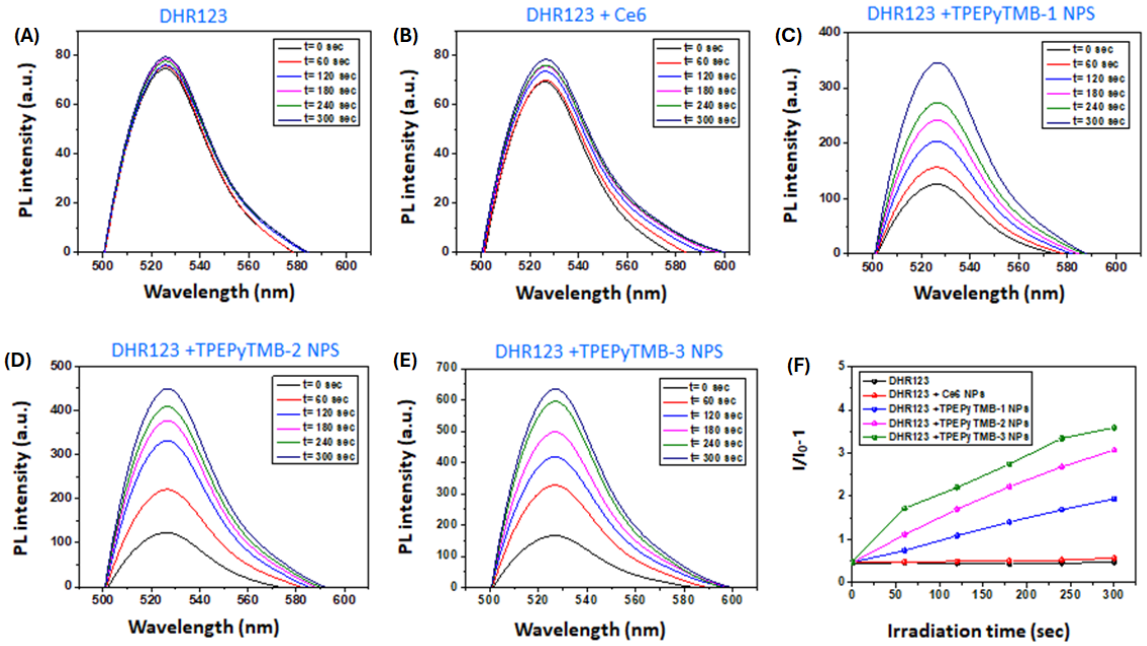

Fig. S17. PL spectra of (a) pure DHR123 (5 μM), (b) DHR123+Ce6 (10 μM), (c) DHR123 +TPEPyTMB-1 NPs (10 μM), (d) DHR123+TPEPyTMB-2 NPs (10μM), (e) DHR123+TPEPyTMB-3 NPs (10 μM) upon white light (100 mW/cm ^{2}) irradiation and (f) relative $O_2^{\cdot-}$ generation efficiency of AIE-PSs NPs and Ce6.

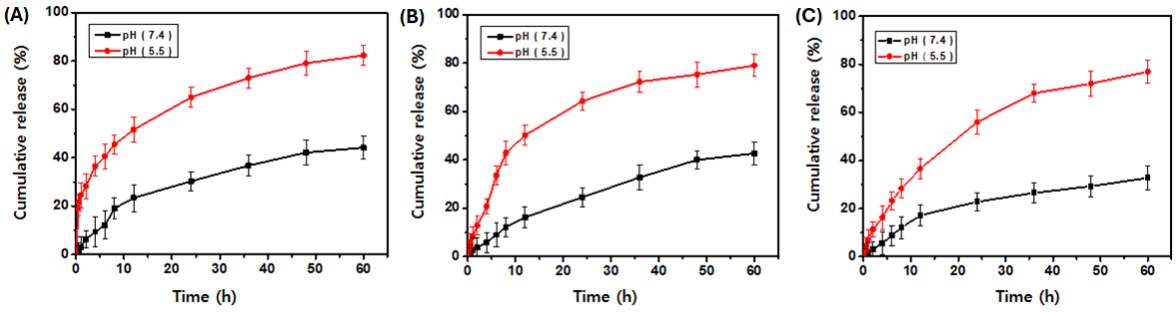

Fig. S18. Release profiles of TPEPyTMB-1, TPEPyTMB-2, and TPEPyTMB-3 PSs from the AIE-PSs NPs under different pH conditions.

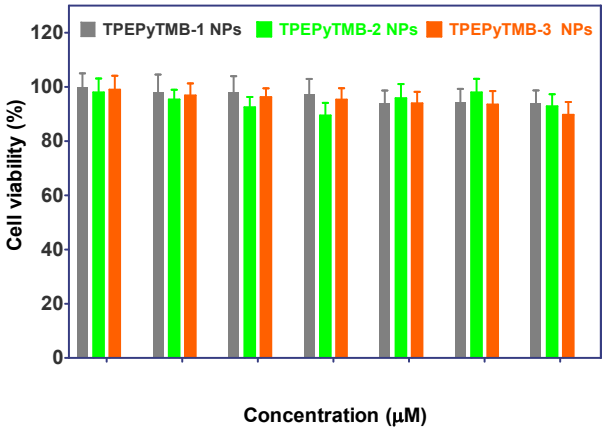

Fig. S19. Cell viability of MCF-7 cells treated with TPEPyTMB-1, TPEPyTMB-2, and TPEPyTMB-3 NPs under dark conditions.

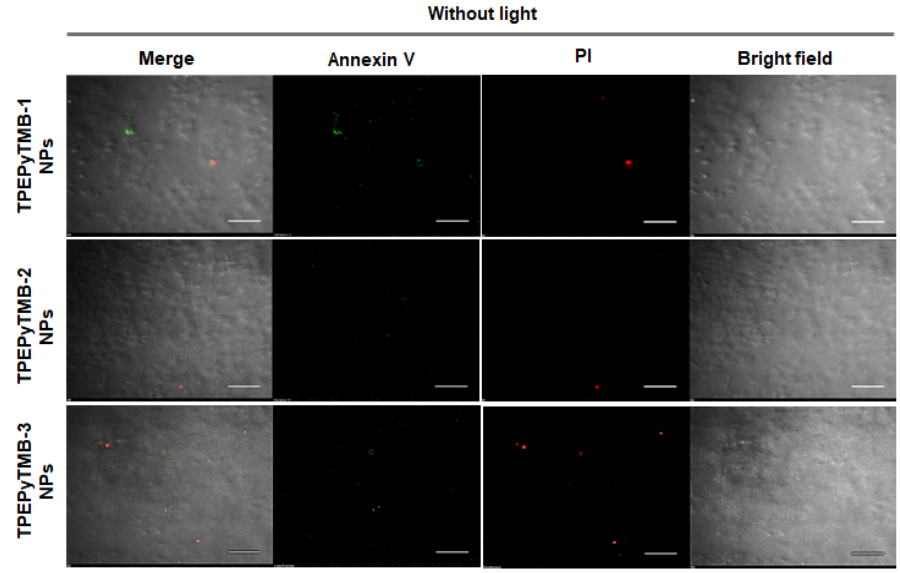

Fig. S20. Confocal microscopic images of apoptosis in MCF-7 cells after 24 h incubation with TPEPyTMB-1, TPEPyTMB-2, and TPEPyTMB-3 NPs of 1 μM under dark conditions in a hypoxic environment. (Scale bar = 100 μm).

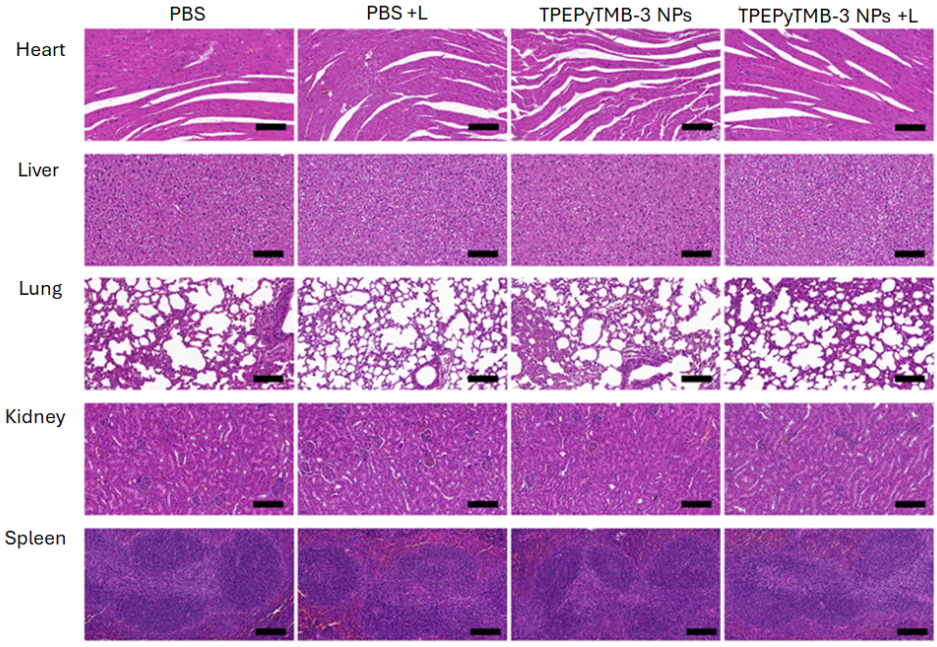

Fig. S21. H&E staining of the major organs of mice at day 14 after treatment with PBS and TPEPyTMB-3 NPs with/without white light irradiation (100 mW/cm^2). Scale bars = 100 μm.

Table S2. Summary of the fluorescence quantum yield (ϕ_F) of previously existing TPE-based photosensitizers

Name	Chemical structure	Fluorescence quantum yield (ϕ_F)	Ref.
TPEDC dots	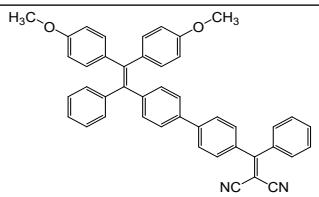	11.2%	2
PTPEDC1 dots	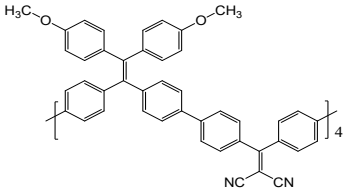	11.9%	2
PTPEDC2 dots	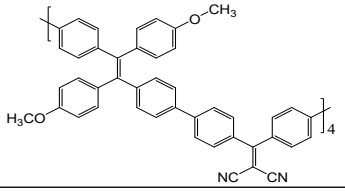	3.1 %	2
TPEPY-SH	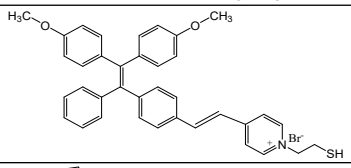	10.3%	3
TTFMN	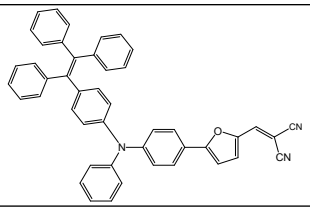	4.3%	4
AIE-Red	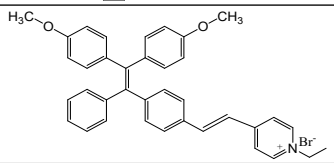	8.1 %	5
TTD	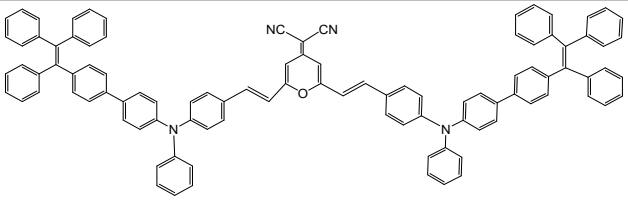	10.1 %	6
TPE-benzothiazole (6)	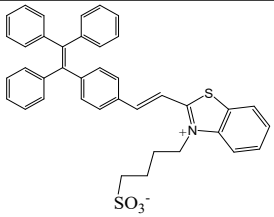	13.2%	7

AP2	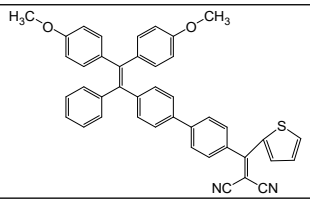	12%	8
AP3	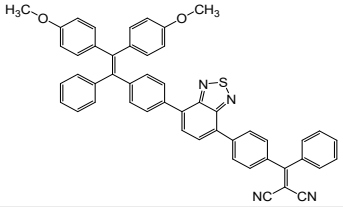	10%	8
TPE-IQ-2O	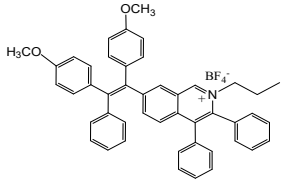	13.1%	9
In this study TPEPyTMB-1 NPs	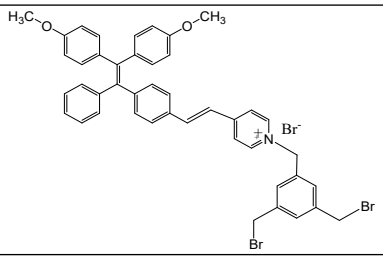	8.49 %	-
In this study TPEPyTMB-2 NPs	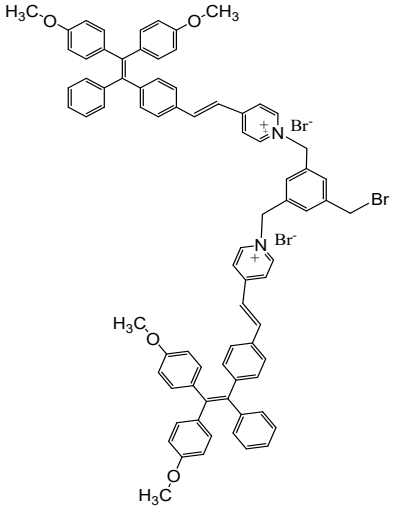	11.81 %	-
In this study TPEPyTMB-3 NPs	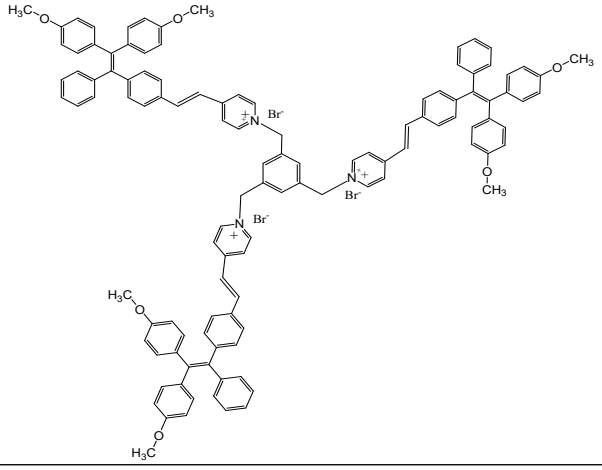	15.08 %	-

Reference:

1. Sauraj et al., Novel aggregation-induced emission-photosensitizers with built-in capability of mitochondria targeting and glutathione depletion for efficient photodynamic therapy, *Nanoscale*, 2023,15, 4882-4892

2. Wang et al., Polymerization-Enhanced Two-Photon Photosensitization for Precise Photodynamic Therapy, *ACS Nano,* 2019, 13, 3, 3095–3105.

3. Zhang et al., AIE-based GSH activatable photosensitizer for imaging-guided photodynamic therapy, *Chem. Commun.*, 2020,56, 10317-10320

4. Kang et al., Good Steel Used in the Blade: Well-Tailored Type-I Photosensitizers with Aggregation-Induced Emission Characteristics for Precise Nuclear Targeting Photodynamic Therapy, Adv. Sci. 2021, 8, 2100524

5. Hu et al., Multicolor monitoring of cellular organelles by single wavelength excitation to visualize the mitophagy process, Chem. Sci.,2018,9,2756–2761

6. Yuan et al., Targeted and image-guided photodynamic cancer therapy based on organic nanoparticles with aggregation-induced emission characteristics, Chem. Commun., 2014, 50,8757.

7. Jayaram et al., In Vitro and in Vivo Demonstration of Photodynamic Activity and Cytoplasm Imaging through TPE Nanoparticles, *ACS Chem. Biol.* 2016, 11, 1, 104–112

8. Wu at al., High Performance Photosensitizers with Aggregation-Induced Emission for Image-Guided Photodyna mic Anticancer Therapy, *Mater. Horiz.*, 2017,4, 1110-1114

9. Gui et al., AIE-active theranostic system: selective staining and killing of cancer cells Chem. Sci., 2017, 8, 1822–1830.